BUTTERWORTH HEINEMANN

Modeling cation/anion–water interactions in functional aluminosilicate structures

Antony J. Richards,*,†,§ Paul Barnes,* David R. Collins,*,‡ Fotis Christodoulos,§ and Simon M. Clark*,‖

*Industrial Materials Group, Department of Crystallography, Birkbeck College, London, U.K.

†British Gas plc, Research and Technology Division, London Research Station, London, U.K.

‡Commission of the European Communities, Joint Research Centre, Institute for Systems Engineering and Informatics, Ispra, Italy

§Molecular Simulations, 240/250 The Quorum, Cambridge, U.K.

‖Daresbury Laboratory, Warrington, U.K.

A need for the computer simulation of hydration/dehydration processes in functional aluminosilicate structures has been noted. Full and realistic simulations of these systems can be somewhat ambitious and require the aid of interactive computer graphics to identify key structural/chemical units, both in the devising of suitable water–ion simulation potentials and in the analysis of hydrogen-bonding schemes in the subsequent simulation studies. In this article, the former is demonstrated by the assembling of a range of essential water–ion potentials. These span the range of formal charges from +4e to −2e, and are evaluated in the context of three types of structure: a porous zeolite, calcium silicate cement, and layered clay. As an example of the latter, the computer graphics output from Monte Carlo computer simulation studies of hydration/dehydration in calcium–zeolite A is presented.

Keywords: water–cation interactions, water–anion interactions, computer simulation, Monte Carlo, zeolite A, tricalcium silicate, kaolinite

Color plates for this article are on pp. 56 and 57.

Address reprint requests to Prof. Barnes, Department of Crystallography, Birkbeck College, London WC1E 7HX, U.K.
Received 17 May 1994; accepted 5 July 1994.

INTRODUCTION

A previous paper[1] outlined a new method for determining water–cation short-range potentials for use with aluminosilicate structures. The method, which is briefly outlined below, was specifically aimed at situations involving highly charged cations in which it was necessary, during the quantum mechanical evaluations, to embed the cation within a cluster of point charges that in effect modeled both the "counterion effect" and the long-range "Madelung" interactions. Using this approach, it became possible to derive realistic formal Si^{4+}–, Al^{3+}–, and Ca^{2+}–H_2O repulsion potential parameters characterized for a number of key aluminosilicate structures.

The aims of the present study were to extend this idea to cover the cases of both cation– and anion–water potentials and, in so doing, to be able to model all relevant water interactions within a wider range of useful aluminosilicate structures. As a result, a set of working potentials has now been identified, spanning a formal charge range from $+4e$ to $-2e$, which can act as an essential "tool kit" for modeling the role of water in the synthesis and function of several basic structures of industrial importance. These structures comprise a zeolite, silicate cement, and layered clay in various hydrated forms.

METHOD

Once a given structural system (and associated water content) has been identified for study, the method consists of the five following basic steps:

Journal of Molecular Graphics 13:28–35, 1995

655 Avenue of the Americas, New York, NY 10010

0263-7855/95/$10.00
SSDI 0263-7855(94)00005-D

1. Energy minimization of the required structure, and extraction of the relevant Madelung parameters
2. Search for a suitable charge cluster around the chosen cation/anion to model the counterion and long-range (Madelung) effects
3. Quantum mechanical evaluation of the interaction of water with the cation/anion surrounded by its charge cluster
4. Quantum mechanical evaluation of the interaction of water with a dummy cation/anion
5. Treatment of data (steps 3 and 4) to produce a working potential and subsequent use in simulations of the chosen hydrated system.

Examples of these steps are illustrated in this article.

In principle the coordinates of experimentally determined structures could be used to evaluate the Madelung energy at the cation/anion site (step 1), although it is preferable to use energy-minimized, or at least "energy-relaxed," structures (i.e., a minimized structure in which certain species remain fixed). This tends to remove any unrealistic sharpness or singularities in the calculations. Ideally, there should be close correspondence between the experimentally determined and energy-minimized/relaxed structures. In the cases given here, this has been achieved using the established methods of energy minimization by Catlow and Mackrodt,[2] in which formal electronic charges are normally used to model the Coulombic interactions with an Ewald summation[3,4] for the long-range electrostatic effect, and a short-range repulsion–attraction term to account for repulsive electron cloud overlap and van der Waals attraction; in addition, this model may be extended to include a description of electronic polarizability using the Shell model[5] and a three-body harmonic bond-bending term[6] to describe directionality of covalency (i.e., Al/Si–O–Al/Si groups). The actual energy-minimization program used was THBREL[7] which uses the Newton–Raphson second derivative method to achieve rapid and stable convergence of energy by the iterative adjustment of atomic positions from an initial trial structure.

The choice of charge cluster (step 2) requires specific crystal chemistry considerations, and is best achieved using molecular graphics: individual examples are given below.

THE CHOSEN STRUCTURES

Sodium–zeolite A; calcium–zeolite A

Zeolites are crystalline aluminosilicates, which occur naturally as minerals or as synthesized in the laboratory, and have a wide variety of uses including catalytic, ion-exchange, and molecular sieving applications.[8] Of the rich variety now available, zeolite A is one of the simpler and more basic zeolites with commercial applications as a water softener in detergents and as a drying agent. Its structure (Color Plate 1a) is based on truncated octahedra known as sodalite or β cages. These are joined together in three dimensions through six four-membered rings to produce a three-dimensional pore system with relatively narrow windows leading to a larger cavity (4.1 Å in diameter) known as the α cage.

The energy minimization of both Ca– and Na–zeolite A employed formal charge potential models, with the framework structure of Pluth and Smith[9] used as the starting configuration. In the case of Na–zeolite A, there are 96 cations distributed at 3 types of site associated with the 8-, 6-, and 4-rings. For an Al:Si ratio of 1.0, the occupancy of the latter site is negligible. Following an approach adopted by Jackson and Catlow,[10] all the 6- and 8-ring sites were filled while the 4-ring sites were left vacant, and in order to maintain charge neutrality the charge on the oxygen atoms was reduced slightly. The final energy-minimized structure was found to be close to the experimental structure. However, in the case of Ca–zeolite A, charge neutrality requires only half the number of cations (i.e., 48 per unit cell), which, according to Pluth and Smith,[9] fill only the 2 sites that reside close to the centers of the 6-membered rings; as there are 128 possible sites per unit cell, their filling was performed by random assignment of the 48 calcium cations among the 128 sites but with the provision that the overall statistical occupancy indicated by Pluth and Smith[9] was maintained, that is, no 6-membered ring is allowed to have more than 1 calcium cation in its proximity (see Color Plate 2a).

Tricalcium silicate cement (C_3S)

Tricalcium silicate[11] is the major component of modern Portland cement; it is also known by its associated mineral name "alite," and by its stoichiometric shorthand "C_3S." Because cement constitutes, by weight after iron/steel, the second largest manufactured commodity today, and because its initial interaction with water is crucial to forming the calcium–silicate–hydrates "C-S-H" that impart binding strength to most of the world's engineering structures, it clearly falls within the remit of an "important functional hydrated structure." A better description of the interactions between C_3S and water would enhance our understanding of the kinetics (acceleration, retardation, poisoning, etc.) of the key topochemical reactions that occur during the introduction of water to C_3S.

The first clear structural elucidation of a C_3S structure was made by Jeffery,[12] using an averaged pseudorhombohedral (R_3m)-true monoclinic (Cm) cell, with minor substitutions for stabilization purposes. It consists of linked columns of silica tetrahedra and approximately octahedrally coordinated calciums, although it can also be alternatively envisaged as orthosilicate ("C_2S") layers sandwiched by a CaO ("C") layer (see Color Plate 1b). In this study the structure published by Golovastikov et al.[13] was used as the starting structure because this solution was based on the pure C_3S material with a $P1$-triclinic cell: The energy minimization of this structure was also performed using THBREL,[7] at constant pressure; energy convergence was rapid, within 30 cycles, all atom shifts being within 0.1 Å. Exploring the environment of the calcium atoms using standard molecular graphic routines[14] shows that both the experimental and minimized structures exhibit two types of both calcium and oxygen coordination:

Ca_I: Sixfold coordinated by oxygens
Ca_{II}: Sevenfold coordinated by oxygens
O_I: Fourfold coordinated by three calciums and one silicon
O_{II}: Sixfold coordinated by six calciums

Kaolinite

The name *kaolinite* refers to the strict single chemical phase, $Al_2Si_2O_9H_4$, pertaining to the mineral "kaolin," which occurs as a natural clay deposit in many locations throughout the world. It has a multitude of industrial uses, such as in papers, rubbers, and paints, but particularly as a basic ingredient in the synthesis of ceramics. Its layered structure,[15–18] depicted in Color Plate 1c, leads to a number of key properties. It consists of neutral aluminosilicate layers, containing Si and Al in tetrahedral and octahedral coordinations, respectively, held together by relatively weak hydrogen bonding; this leads to its well-known partial disorder in the stacking of the layers, a property that varies considerably between different kaolin types.

Another feature that has attracted much interest concerns the precise location of hydrogen atoms, which has been the subject of much controversy.[15–17,19] There are two types of hydrogen environment in kaolinite, namely (1) inner surface hydrogens, which are located at the surface of the layers and are involved in interlayer hydrogen bonding with basal oxygen atoms at the surface of the adjacent layer, and (2) inner hydrogens, which are located within the individual layers, both of which are illustrated in Color Plate 1c. Previous neutron diffraction studies[15–17] reported conflicting orientations for the inner surface hydroxyl groups. A subsequent X-ray diffraction study[18] determined an accurate nonhydrogen atom structure in space group $C1$. The work on kaolinite reported in this study uses the nonhydrogen structure of Bish and Von Dreele with hydrogen positions that have been determined using energy minimization procedures.[19]

Because of difficulties in modeling the relatively weak interlayer bonding referred to above, it was not feasible to perform a full energy minimization on kaolinite. Instead the nonhydrogen atoms (Si, Al, and O) were held fixed[18] while the hydrogen atoms were allowed to relax. This approach produces energy-minimized hydrogen atom positions within a reliable experimentally determined structure. Full formal charges were placed on all atoms except those of the hydroxyl groups, which used $-1.426e$ and $0.426e$ for the O and H atoms respectively, giving a net OH charge of $-1e$ and reproducing the dipole moment of a hydroxyl group.[20] The intramolecular hydroxyl interactions were modeled using a Coulombic-subtracted Morse function[20] while the interlayer hydrogen bonds were treated as purely electrostatic. The orientations of the hydroxyl groups due to energy relaxation of the hydrogen atoms are shown in Color Plate 1c. It is seen that all the inner surface hydroxyl groups are found to point almost perpendicularly to the layers. In fact each inner surface hydroxyl points toward a basal oxygen atom in the adjacent layer, thus indicating the formation of interlayer hydrogen bonding. The inner hydroxyl is shown to be directed toward the vacant octahedral site.

THE SEARCH FOR SUITABLE CHARGE CLUSTERS

As mentioned previously, the method (step 2) requires a consideration of the cation/anion environment within the chosen structure in relation to any advancing water molecules during a given state of hydration. This is a key step in the method: the cation/anion may be highly charged and in practice the advancing water molecule is partly shielded from its high field by the surrounding counterions. If derived potentials are to be realistic and truly representative of the structures under study, the quantum mechanical evaluations must take this effect into account; furthermore, there is an added hope that, in so doing, this approach will impart some transferability to the potentials across related structures. The method then requires modeling the counterion effect by devising a model cluster of point charges surrounding the cation/anion that can mimic the local electrostatic environment for the quantum mechanical evaluations. This is best done using a combination of chemical intuition and molecular graphic aids; the space around the cation/anion is searched using standard molecular graphics routines,[14] starting with the cation/anion at the center of view, and the search radius is increased until the first and simplest (chemically) sensible fragment, with an overall counterion nature, is achieved. In the simplest and most trivial case of silicate/aluminate tetrahedra, this is obtained with just one shell of four negative point charges tetrahedrally surrounding the Si^{4+}/Al^{3+} cation; in the more complex cases (e.g., Ca–zeolite A; kaolinite), second and even third shells may need to be brought into play. The 10 cases under consideration in this study, along with the counterion clusters, are illustrated in Color Plate 1d.

Once the charge cluster has been chosen in the geometric sense, the magnitudes of the individual point charges, q_i, need to be determined. Again for the most trivial case of silicate/aluminate tetrahedra this becomes a straightforward equality between the Madelung field, E_m, and the sum of four equal electrostatic contributions from the point charges:

$$E_m = \Sigma\, q_i/r \quad (i = 1 \text{ to } 4) \tag{1}$$

where r is the distance between each charge and the center of the cluster (Color Plate 1d). In the particular case of Si^{4+} in quartz and zeolite A (Table 1) a value of $q_i = -1.4e$ is obtained; thus it is seen that the formal cation plus charge cluster is not neutral overall $[+4e - (4 \times 1.4e) = -1.6e]$ as expected because the role of the charge cluster is to mimic the net effect of both the local counterions and the overall lattice. In the case of multiple shell fragments, an intuitive element must be included in the method because there is often some choice in how to define the cluster. For example, in the more extreme example of OH^- in kaolinite the fragment consists of three shells (if we collapse the O and H in OH^- as one effective atom) representing three types of counterions (Si^{4+}, Al^{3+}, and OH^-) so that the determining equation becomes

$$E_m = \sum_{i=1}^{i=7} q_i/r_i = 2q_{Al}/r_{Al} + 2q_{OH}/r_{OH} + 3q_O/r_O \tag{2}$$

where q_{Al}, q_{OH}, and q_O are the cluster point charges representing, respectively, the original Al^{3+}, OH^-, and O^{2-} counterions, and r_{Al}, r_{OH}, and r_O are their respective distances from the OH^- anion center. The choice of how to

Table 1. Summary of charge cluster parameters used for deriving various ion–water interactions in the chosen structures

Ion	Formal charge	System	Cluster size	Madelung energy (eV)	Cluster charges (e)
Silicon	+4	Quartz/zeolite A	4	−200	Oxygen: −1.4 (×4)
Aluminum	+3	Quartz	4	−200	Oxygen: −1.6 (×4)
Calcium	+2	Zeolite A	12	−31.5	Oxygen: −1.6 (×6)
					Silicon: 4.0 (×3)
					Aluminum: 3.0 (×3)
		Tricalcium silicate	6	−41.5	Oxygen: −1.2 (×6)
		Tricalcium silicate	7	−41.3	Oxygen: −1.0 (×7)
Sodium	+1	Zeolite A	12	−16.8	Oxygen: −1.3 (×6)
					Silicon: 4.0 (×3)
					Aluminum: 3.0 (×3)
		Zeolite A	16	−22.2	Oxygen: −1.4 (×8)
					Silicon: 4.0 (×4)
					Aluminum: 3.0 (×4)
Hydroxyl	−1	Kaolinite	9	−25.9	Oxygen: −1.5 (×3)
					Aluminum: 3.0 (×2)
					Oxygen (OH): −1.4 (×12)
					Hydrogen: 0.4 (×3)
Oxygen	−2	Tricalcium silicate	4	−51.7	Calcium: 0.9 (×3)
					Silicon: 1.8 (×1)
		Tricalcium silicate	6	−40.3	Calcium: 0.7 (×6)

vary these three species is dictated by the following considerations: that the net sign of the quantities on both sides of Eq. (2) must be the same; that one achieves this by first altering the innermost shell and using formal species charges for the remaining shells, and so on, until a sensible equality to Eq. (2) is achieved. In cases in which there are shells of alternating charge sign it is problematic, unless one adopts a consistent strategy such as this, to obtain chemically unrealistic charges that nevertheless still reproduce the correct Madelung field. The appropriate Madelung fields used are listed in Table 1, which also specifies the derived charge clusters for the cases illustrated in Color Plate 1d: it is obvious from Table 1 which point charges have remained with their formal values and which have been varied in the above manner.

RESULTS

Assembling suitable ion–water potentials

The first use of the above data has been to derive effective potentials for studying ion–water interactions in the chosen structures. As already explained, quantum mechanical evaluations are made for the interaction of water with the cation/anion surrounded by its charge cluster, and then compared with a dummy cation/anion analog of the same complex. This procedure is expressed algebraically in the following two equations:

$$E_a = E_{w\text{-}fi}^{electro} + E_{w\text{-}cc}^{electro} + E_w^{pol} + A_{w\text{-}fi}^{rep} \cdot \exp(-r/b) \quad (3)$$

$$E_b = E_{w\text{-}di}^{electro} + E_{w\text{-}cc}^{electro} + E_w^{pol} \quad (4)$$

where the superscripts describe the type of interaction (electro, electrostatic; pol, polarization; rep, short-range repulsion) and the subscripts indicate the actual interacting species (fi, formal ion; di, dummy ion; w, water; cc, charge cluster) and A and b are constants for the given water–cation pair. On subtraction, $E_a - E_b$, the first three terms will almost exactly cancel to leave just the exponential term, which describes the short-range repulsion between the shielded ion and the approaching water molecule. The values obtained for $E_a - E_b$ as a function of ion–water separation (r) are given in Table 2 for all six ions under study (Si^{4+}, Al^{3+}, Ca^{2+}, Na^+, OH^-, and O^{2-}) distributed among the three chosen structural types. In the case of Na^+ and Ca^{2+} more than one entry is given corresponding to the differing coordinations found for these ions within the chosen structure. These results are illustrated with one graphic example (Figure 1); this first shows (Figure 1a) the close agreement between the two sets of extracted repulsion energies, $E_a - E_b$, for Na^+ in two different environments; that is, Na^+ surrounded, respectively, by a 12-charge cluster (for the 6-ring Na^+ site in zeolite A) and a 16-charge cluster (for the 8-ring Na^+ site in zeolite A). These data are then individually least-squares fitted to the Born–Mayer short-range repulsion term $[A \cdot \exp(-r/b)]$. A graphic example is given, again for Na^+ in zeolite A (Figure 1b) for the 8-ring site, showing the goodness of fit. In some cases, a small negative overshoot occurs in $E_a - E_b(r)$ which can be treated as a residual error of the method and least-squares fitted out using a negative correction term of the form $-b/r^6$. A list of the parameters obtained for all ions considered is given in Table 3.

Once a suitable electrostatic charge model for the water is chosen, Table 3 in effect provides an essential potential

Table 2. Values obtained for the repulsion energies ($E_a - E_b$) as a function of ion–water distance, for the six ions under study.

Ion (formal charge):	Si (4+)	Al (3+)	Ca (2+)	Ca (2+)	Ca (2+)	Na (1+)	Na (1+)	OH (1−)	O (2−)
Cluster size:	4	4	12	7	6	16	12	9	6
Distance (Å)	$E_a - E_b$ (eV)								
1.4	18.917	9.541	19.719	24.046	23.923	8.408	8.047	10.896	19.526
1.5	15.704	6.230	—	17.708	17.579	5.544	5.268	8.523	16.247
1.6	12.972	3.795	9.397	13.051	12.938	3.645	3.421	6.506	13.094
1.7	10.222	2.041	—	9.571	9.497	2.388	2.202	4.574	10.265
1.8	7.382	0.919	4.203	6.932	6.915	1.558	1.402	2.937	7.900
1.9	4.708	0.309	—	4.925	4.975	1.011	0.879	1.685	6.031
2.0	2.558	0.032	1.768	3.417	3.529	0.650	0.542	0.768	4.594
2.1	1.141	−0.073	—	2.311	2.466	0.415	0.326	0.116	3.500
2.2	0.388	−0.101	0.578	1.525	1.697	0.262	0.190	−0.324	2.670
2.3	0.065	−0.098	—	0.983	1.148	0.162	0.106	−0.593	2.042
2.4	−0.046	−0.082	—	0.621	0.762	0.098	0.054	−0.729	1.565
2.5	−0.069	−0.066	0.168	0.385	0.495	0.057	0.023	−0.771	1.203
2.6	—	—	—	0.233	0.314	0.024	0.003	−0.749	0.929
2.7	—	—	0.046	0.138	0.194	0.015	−0.008	−0.688	0.720
2.8	—	—	—	0.079	0.116	0.006	−0.013	−0.609	0.561
2.9	—	—	—	0.044	0.068	−0.001	−0.015	−0.523	0.439
3.0	−0.017	−0.017	0.009	0.022	0.037	−0.004	−0.016	−0.438	0.346
3.1	—	—	—	0.010	0.019	−0.007	−0.015	−0.358	0.274
3.2	—	—	−0.002	0.003	−0.008	−0.008	−0.015	−0.287	0.218
3.3	—	—	—	−0.001	0.002	−0.008	−0.012	−0.224	0.174
3.4	—	—	—	−0.002	0.000	−0.007	−0.011	−0.170	0.140
3.5	−0.003	−0.005	−0.005	−0.003	−0.002	−0.007	−0.010	−0.126	0.112
4.0	−0.001	−0.003	−0.004	−0.002	−0.002	−0.004	−0.005	0.004	0.040
4.5	−0.001	−0.002	—	—	—	—	—	0.040	—
5.0	0.000	−0.001	−0.001	−0.001	0.001	−0.002	−0.002	0.043	0.005
6.0	—	—	—	—	—	—	—	0.037	—
10.0	—	—	—	—	—	0.000	0.000	—	—

"tool kit" for modeling the role of water in the chosen structures. For example, in the study described in the next section, four parameters from Table 3 (Si^{4+}–, Al^{3+}–, Ca^{2+}–, and O^{2}–H_2O repulsive potential parameters) were combined[21] with the TIP4P point charge model[22] to represent the electrostatic interactions with water; these are expressed in the following form:

$$V_i = A_i \cdot \exp(-r_i/b_i) + \sum_j (n_i e) \cdot (q_j e)/r_{ij} \quad (5)$$

where A_i and b_i are the parameters for the ith ion carrying a formal charge of $n_i e$; r_i represents the separation of the ith ion from the water molecule; $q_j e$ are the point charges used with the TIP4P water–water potential; and r_{ij} is the distance between the ith ion and the jth point charge of the TIP4P water model.

A simulation study of dehydration in calcium–zeolite A

The above potentials were assembled in order to initiate a simulation study of hydration/dehydration in Ca–zeolite A, a process that has relevance to the synthesis of the zeolite and to its activation as a drying agent. There is experimental evidence (density and thermogravimetric measurements[23]) to suggest that zeolite A can accommodate a maximum of about 27 water molecules per pair of α and β cages. It has been further speculated[24] that, of these water molecules, about 20 are contained within the (larger) α cage with the remainder distributed within the (smaller) β cages. Two types of Monte Carlo (grand canonical and canonical) simulation studies have been performed: the first was to check this division of water molecules between the two types of cage, while the second was concerned with a more detailed investigation of water-binding sites during the final stages of dehydration. In both cases the simulation cell was based

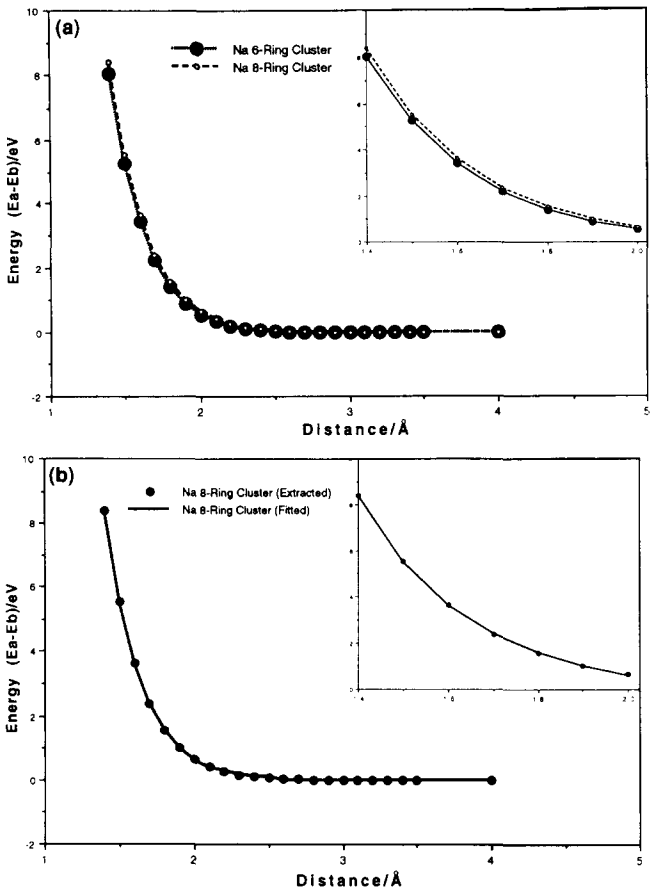

Figure 1. (a) Comparison of short-range repulsion energy terms obtained for Na–H_2O interactions modeled using the 6-ring (12-point charge cluster) site for the Na^+ cation (large filled circles), and using the 8-ring (16-point charge cluster) site for the Na^+ cation (small open circles). The inset shows a magnified region of the curve to show the close agreement. (b) Example of the smooth short-range repulsion energy curve obtained for Na–H_2O interactions modeled for the 8-ring cluster in the sodium–zeolite A structure [datum points = $E_a - E_b$; continuous curve = least-squares fit to $A_i \exp(-r_i/b_i)$].

on the Ca–zeolite A crystallographic unit cell (i.e., 8 pairs of α and β cages) containing 624 non-water-related atoms (96 Al, 96 Si, 384 O, and 48 Ca) with "quasirandom filling" of the 128 possible cation sites by the 48 calcium cations available (Color Plate 2a). The standard minimum image convention and periodic boundary condition were employed as required. Because these simulations were primarily aimed at representing the final stages of dehydration, the calcium cations were constrained to the above-known final positions with no flexing of the lattice framework; both these constraints are to be removed[25] in future simulations of the full dehydration process from the fully hydrated state, thus permitting complete hydration of the cations and interaction with the framework, as is known to occur from combined X-ray diffraction and absorption spectroscopy studies[26,27] of other zeolites.

The first set of simulations utilized the CERIUS[28] molecular modeling software for materials research. First, the zeolite framework was built from the unit cell, space group, and asymmetric unit coordinates using the standard crystal-building module. The cation sites were determined using a "disorder function" that performed the quasirandom filling procedure described earlier. A "Connolly" surface,[29,30] which indicates available space by means of rolling a "tracker molecule" with a probe radius approximately equivalent to that of a water molecule over the van der Waals surface of the framework, was calculated. It can be seen (Color Plate 2b) that, whereas the α cages are readily accessible, there is only limited access in the β cages for water molecules: this limited access results from the cations blocking the six-membered ring "entry doors."

Once the simulation structure has been built, a force field was assembled to describe both framework–water and water–water interactions. This was constructed by combining the potential defined in Eq. (5) with the parameters of Table 3 and the TIP4P water geometry/potential.[22] The CERIUS software, however, rather than using exponential forms $[A_i \cdot \exp(-r_i/b_i)$ as in Eq. (5)] for repulsive potentials, utilizes parameters based on the well representation as defined in Eq. (6):

$$V_i = \epsilon_i \cdot \exp[-\gamma(1 - r_i/\sigma_i)] \quad (6)$$

Equation (6) is a general well representation employing a well shape factor, γ normally with a value between 10 and 14 and set to 12 in this study. Equation (7) is the specific CERIUS representation for the Lennard–Jones 12-6 form as used in the TIP4P potential,

$$V_i = \epsilon_i [(\sigma_i/r_i)^{12} - 2(\sigma_i/r_i)^6] \quad (7)$$

The parameters ϵ_i and σ_i retain their usual meanings of well depth and equilibrium separation, respectively. The resultant force field for this study is detailed in Table 4.

Simulations were performed for ambient conditions (300 K and 1 atm) with 10^7 simulation steps using CERIUS-Sorption, which utilises a grand canonical ensemble. In this description the temperature and partial pressure of the sorbate are held fixed while the number of sorbate molecules in the structure is increased (or "loaded" in common terminology) as a result of random sorbate molecule creation/destruction/translation/rotation events performed with acceptance/rejection decisions dictated in accordance with the standard Monte Carlo condition. This procedure continues until equilibration in the loading is achieved. In this case convergence was attained after 10^7 configurations using a DEC-alpha machine at simulation rates of around 10^5 configurations per CPU hour. This resulted in a loading (on average) of 31.6 molecules per pair of α and β cages. A second such simulation was then performed but with access to the (smaller) sodalite cages blocked. This had the effect of reducing the maximum water loading to 28.9 molecules per pair of α and β cages. These two simulations predict that Ca–zeolite A can accommodate a maximum of 32 water molecules (Color Plate 2c), with approximately 29 of these being in the α cage: this result compares favorably with the experimental results.[23,24]

These trends are illustrated in Color Plates 2 and 3: The average site population of water molecules over the whole simulation is illustrated by means of either a dot-density map (Color Plate 2d), each dot representing one Monte

Table 3. Ion–water repulsion potential parameters for the six ion types considered.[a]

Ion	Formal charge	System	Cluster size	A (eV)	b (Å)
Silicon	+4	Quartz/zeolite A	4	14 780	0.287
Aluminum	+3	Quartz/zeolite A	4	18 650	0.205
Calcium	+2	Zeolite A	12	6 190	0.261
		Tricalcium silicate	7	5 360	0.297
		Tricalcium silicate	6	3 950	0.303
Sodium	+1	Zeolite A	16	3 140	0.244
		Zeolite A	12	3 830	0.238
Hydroxyl	−1	Kaolinite	9	12 340	0.273
Oxygen	−2	Tricalcium silicate	6	2 120	0.348

[a]Obtained by least-squares fitting of the $E_a - E_b$ data from Table 2.

Carlo occurrence, or the equivalent color-coded mass-density plots (Color Plate 3). These figures illustrate a number of points: first, that water traffic between cages is limited and in particular that the α cages are indeed populated at the expense of the smaller β cages; the presence of "hot spots" indicates either reduced water traffic, evident inside the channels connecting the cages or surprisingly near the center of the α cages, or specific hydrogen bonding to the framework oxygens to the exclusion of bonding to the cations.

The final stages of dehydration were simulated[21,23] with canonical Monte Carlo sampling statistics using program codes written specifically to exploit the Cray/CONVEX architecture at the University of London Computer Centre (ULCC). A final dehydration sequence of 20, 14, 10, 6, and 2 water molecules per α cage was set up for temperatures of 300, 400, 500, 600, and 700 K, respectively, because X-ray/neutron diffraction data were also available[21,23] on this system at these same temperatures. Typically 70 000 configurations were used to equilibriate each sequence stage, with ensemble averages taken over a further 7 000 configurations. As the water population decreases, specific hydrogen bonding of water molecules to the framework oxygens becomes increasingly apparent: in fact, four such types of hydration site were identified[21,23] and associated with the 4-, 6-, and 8-rings of the α cages, respectively, their populations reflecting the strength of the individual hydrogen bond and the degree of dehydration.

CONCLUSIONS

Interactive computer graphics provide an essential tool for the production of lattice-effective water–ion potentials, and in the subsequent use of these potentials for simulation studies of hydration/dehydration processes in functional zeolites. In the former case, it is found that the identification of a suitable chemical cluster surrounding a chosen cation or anion is required as a means of devising a (related) charge cluster that can effectively model the counterion and lattice effects during quantum mechanical evaluations of the water–ion interactions. In this way it has been possible to assemble effective pair potentials for a range of ions encountered in three types of functional structures (a porous zeolite, calcium-silicate cement, and layered clay) and that span a range of formal charges from $+4e$ to $-2e$. The use of such potentials has been demonstrated in a nontrivial computer simulation study of water packing and subsequent dehydration in Ca–zeolite A: here, the use of interactive computer graphics was required to study both the initial water packing into the zeolite structure as well as to identify

Table 4. Potential interaction parameters for the various ion–water pairs under study, according to the various representations given in Equations (5) to (7)

Interacting pair	Nature of non-electrostatic part of potential	Species	Electrostatic charge on species	Well depth ϵ (kcal/mol)	Equilibrium separation σ (Å)	Well shape factor γ
H_2O–Si	Repulsive-exponential	Si[a]	$+4e$	2.0932	3.444	12
H_2O–Al	Repulsive-exponential	Al[a]	$+3e$	2.6413	2.460	12
H_2O–Ca	Repulsive-exponential	Ca[a]	$+2e$	0.8766	3.132	12
H_2O–O	Repulsive-exponential	O[a]	$-2e$	0.3004	4.176	12
H_2O–H_2O	Lennard-Jones 12-6	O	0[b]	0.1550	3.540	—
		H	$+0.52e$[b]			
		Dummy	$-1.04e$[b]			

[a]In the case of ion–water interactions, formal charge values are used for the ions and partial charges on the water as described in the TIP4P model[b]; also, a well-shaping factor, γ, is used.

[b]In the case of water–water interactions, the pure TIP4P potential[22] is used: this employs partial charges of 0 and $0.52e$, respectively, on the oxygen and hydrogen centers with the latter displaced 0.9572 Å from the oxygen and describing an HOH angle of 104.52°; charge neutrality is obtained using a dummy ion with a charge of $-1.04e$ placed on the HOH bisector at a distance of 0.15 Å from the oxygen.

favored hydrogen bond configurations that repeatedly form during a Monte Carlo simulation of the final dehydration sequence. It is apparent from these studies that even more ambitious simulations can now be attempted, such as cation exchange and relocation in zeolites for which mobile cations and distorted/defective aluminosilicate frameworks must be permitted for complete realism. Application object-oriented program codes will become increasingly important[25] in these pursuits, including versatile interactive computer graphics.

ACKNOWLEDGMENTS

SERC/ULCC (Dr. J. Altmann) are acknowledged for mainframe computing resources, CHEMX and CERIUS for visualization and molecular modeling software, respectively, and British Gas (Drs. D. Puxley and G. Squire) and Birkbeck College (Mr. M. Vickers) for their various supporting activities.

REFERENCES

1 Aloisi, G., Barnes, P., Catlow, C.R.A., Jackson, R.A., and Richards, A.J. *J. Chem. Phys.* 1990, **93,** 3573–3579
2 Catlow, C.R.A. and Mackrodt, W.C. *Computer Simulation of Solids. Lecture Notes in Physics No. 166* (C.R.A. Catlow and W.C. Mackrodt, Eds.). Springer-Verlag, Berlin, 1982, Ch. 1
3 Ewald, P.P. *Ann. Physik.* 1921, **64,** 253–287
4 Tosi, M.P. *Solid State Phys.* 1964, **16,** 1–120
5 Dick, B.G. and Overhauser, A.W. *Phys. Rev.* 1958, **112,** 90–103
6 Sanders, M.J., Leslie, M., and Catlow, C.R.A. *J. Chem. Soc. Chem. Commun.* 1984, **112,** 1271–1273
7 Leslie, M.L. *SERC Daresbury Laboratory Technical Report.* Daresbury Laboratory, Warrington, U.K., 1993 (in preparation)
8 Breck, D.W. *Zeolite Molecular Sieves: Structure, Chemistry and Use.* John Wiley & Sons, London, 1974
9 Pluth, J.J. and Smith, J.V. *J. Am. Chem. Soc.* 1983, **105,** 1192–1195
10 Jackson, R.A. and Catlow, C.R.A. *Mol. Simul.* 1988, **1,** 207–224
11 Barnes, P. *Structure and Performance of Cements.* Applied Science Publishers, London, 1983
12 Jeffery, J.W. *Acta Cryst.* 1952, **5,** 26–35
13 Golovastikov, N.L., Matveeva, R.G., and Belov, N.V. *Sov. Phys. Cryst.* 1975, **20,** 441
14 Richards, A.J., Maginn, S., Leusen, F.J., and Bick, A. *Data Visualization in Molecular Science.* (J.E. Bowie and A.J. Olson, Eds.) Addison-Wesley, Reading, MA, 1995, Ch. 9
15 Adams, J.M. *Clay Clay Miner.* 1983, **31,** 353–356
16 Suitch, R.A. and Young, P.R. *Clay Clay Miner.* 1983, **31,** 357–366
17 Young, R.A. and Hewat, A. *Clay Clay Miner.* 1988, **36,** 225–232
18 Bish, D.L. and Von Dreele, R.B. *Clay Clay Miner.* 1989, **37,** 289–296
19 Collins, D.R. and Catlow, C.R.A. *Acta Cryst.* 1991, **B47,** 678–682
20 Saul, P., Catlow, C.R.A., and Kendrick, J. *Philos. Mag.* 1985, **B51,** 107–177
21 Richards, A.J., Barnes, P., Tarling, S.E., and Aloisi, G. *Mol. Simul.* 1992, **9,** 311–318
22 Jorgensen, W.L., Chandrasekhar, J., and Madura, J.D. *J. Chem. Phys.* 1983, **79,** 926–935
23 Richards, A.J. Ph.D. thesis, University of London, 1992
24 Dyer, A. *An Introduction to Zeolite Molecular Sieves.* John Wiley & Sons, Chichester, U.K. 1988
25 O'Connor, D.J. and Barnes. private communication (1994)
26 Dooryhee, E., Greaves, G.N., Steel, A.T., Townsend, P., Carr, S.W., Thomas, J.M., and Catlow, C.R.A. *Faraday Disc. Chem. Soc.* 1990, **89,** 119–136
27 Dooryhee, E., Catlow, C.R.A., Couves, J.W., Maddox, P.J., Thomas, J.M., Greaves, G.N., Steel, A.T., and Townsend, P. *J. Phys. Chem.* 1991, **95,** 4514–4521
28 *CERIUS: Molecular Modeling Software for Materials Research.* Molecular Simulations, Inc., Burlington, MA, U.S.A., and Cambridge, U.K.
29 Connolly, M.L. *Science* 1983, **221,** 709–713
30 Connolly, M.L. *J. Appl. Cryst.* 1983, **16,** 548–558